Mon. Not. R. Astron. Soc. 000, 000–000 (0000) Printed le 21 janvier 1999 (MN LATEX style file v1.4)

Galaxy Clustering at $z \sim 2$ and Halo Radii

B. F. Roukema[1,2,3], D. Valls-Gabaud[2,4], B. Mobasher[5] and S. Bajtlik[1]

[1] *Nicolaus Copernicus Astronomical Center, ul. Bartycka 18, 00-716 Warsaw, Poland*
[2] *UMR CNRS 7550, Observatoire de Strasbourg, 11 rue de l'Université, 67000 Strasbourg, France*
[3] *Inter-University Centre for Astronomy and Astrophysics, Post Bag 4, Ganeshkhind, Pune, 411 007, India*
[4] *Royal Greenwich Observatory, Madingley Road, Cambridge CB3 0EZ, UK*
[5] *Astrophysics Group, Blackett Laboratory, Imperial College, Prince Consort Rd, London SW7 2BZ, UK*
Email: boud@iucaa.ernet.in, dvg@astro.u-strasbg.fr, b.mobasher@ic.ac.uk, bajtlik@camk.edu.pl

le 21 janvier 1999

ABSTRACT

The amplitude of the angular two-point galaxy auto-correlation function $w(\theta)$ for galaxies at $z \sim 2$ is estimated for galaxies in the Hubble Deep Field by using a $U < 27$ complete sub-sample. The U-band selection ensures little contamination from $z > 2.5$ galaxies, while photometric redshifts minimise the contribution from low redshift galaxies.

(i) It is confirmed that the amplitude of the correlation can be corrected for the integral constraint (lack of large scale variance) without having to make assumptions about the shape of the correlation function and by avoiding the introduction of linear error terms. The estimate using this technique is $w(\theta \approx 5'') = 0.10 \pm 0.09$. Estimators which assume a power law of a given slope and include linear error terms would double this value.

(ii) If the biases introduced in faint galaxy selection due to obscuration by large objects are not corrected for by masking areas around them, then the estimate would be $w(\theta \approx 5'') = 0.16 \pm 0.07$.

(iii) The effective (three-dimensional) galaxy pair separation at $5''$ and this redshift range is $\approx 25\mathrm{h}^{-1}$ kpc$-250\mathrm{h}^{-1}$ kpc, so the correction to the spatial correlation function $\xi(r)$ due to exclusion of overlapping galaxy dark matter haloes should be considered. For clustering stable in proper units in an $\Omega = 1, \lambda = 0$ universe, our $w(5'')$ estimate (a) implies a present-day correlation length of $r_0 \sim 2.6^{+1.1}_{-1.7}\mathrm{h}^{-1}$ Mpc if halo overlapping is ignored, but (b) for a present-day correlation length of $r_0 = 5.5\mathrm{h}^{-1}$ Mpc implies that a typical halo exclusion radius is $r_{\mathrm{halo}} = 70^{+420}_{-30}\mathrm{h}^{-1}$ kpc. For $\Omega_0 = 0.1, \lambda_0 = 0.9$, the corresponding values are (a) $r_0 \sim 5.8^{+2.4}_{-3.9}\mathrm{h}^{-1}$ Mpc and (b) $r_{\mathrm{halo}} < 210\mathrm{h}^{-1}$ kpc (1σ upper limit).

(iv) The decreasing correlation period (DCP) of a high initial bias in the spatial correlation function is not detected at this redshift. For an $\Omega = 1, \lambda = 0$ universe and stable clustering in proper units, possible detections of the DCP in other work would imply that the values of ξ at redshifts greater than $z_t = 1.7 \pm 0.9$ would be $[(1+z)/(1+z_t)]^{2.1 \pm 3.6}$ times their values at z_t, which is consistent with our lack of a detection at $z \sim 2$.

Key words: cosmology: theory—galaxies: formation—galaxies: clusters: general—galaxies: distribution—cosmology: observations

1 INTRODUCTION

Structure in the Universe as represented by visible galaxies is commonly represented by the two-point spatial auto-correlation function, $\xi(r)$. This can be approximately parametrised as a power law

$$\xi(r) = (r_0/r)^{\gamma} \quad (1)$$

where r are is the spatial separation of galaxy pairs, r and r_0 are expressed in comoving coordinates and γ represents the approach to homogeneity at large length scales (e.g. Groth & Peebles 1977). For a recent review of the galaxy correlation function, see Peacock (1997).

Since the major epoch of star formation in the Universe seems to have taken place at $z \sim 1 - 2$ (Madau et al. 1996), this is a particularly interesting period. It would be useful

to observationally estimate ξ at this epoch in order to link gravitational theory with the study of luminous objects.

Villumsen, Freudling & da Costa (1997) have already made an estimate of the projected, angular two-point autocorrelation function, $w(\theta)$, (where θ is the angle separating two galaxies) and hence ξ, for galaxies in the Hubble Deep Field (hereafter, HDF; Williams et al. 1996), to median redshifts up to $z_{\rm med}\approx$ 1.9 from an I-band selected sample. Several recent estimates for ξ have also been made for both higher redshift objects (Giavalisco et al. 1998 at $z \sim 3$; Miralles, Pelló & Roukema (1999) 1998 in the HDF at $2.5 < z < 4.5$) and for lower redshift galaxies (Connolly, Szalay & Brunner 1998 in the HDF at $z < 1.6$).

An improvement on the Villumsen et al. estimate should be possible by using (i) a U-band selected sample to remove nearly all galaxies at redshifts $z \gtrsim 2.5$, and (ii) photometric redshift redshift estimation on this sample to remove most galaxies at both lower and higher redshifts than $1.5 \lesssim z \lesssim 2.5$.

This is the option chosen here, using Mobasher & Mazzei's (1998) U-selected sample of HDF galaxies, dominated by ellipticals and starburst galaxies at $z \sim 2$ (§2). Although galaxies selected in U at $z \sim 2$ are selected in rest-frame wavelengths which do not correspond to those in which galaxies in typical surveys are selected, the high rate of star formation at this epoch implies that the galaxy mix may not be too different from other samples.

As in Connolly et al. (1998) and Miralles et al. (1998), w is estimated in a redshift range limited by photometric redshifts (§3) and Limber's equation [equation (7)] is used to consider interpretation in terms of the spatial correlation function ξ (§3.2).

In addition, (i) the estimate of w is made without having to make a prior assumption about the shape and slope of the correlation function (§3.1) and by avoiding introduction of linear terms in the correction for the integral constraint; and (ii) the effect of bias introduced in regions of sky obscured by bright objects is demonstrated (§3.1.2).

The word 'bias' in the previous sentence is used in its general sense. Since the primary aim of this paper is observational estimation, galaxy-to-matter bias (e.g. Ostriker 1993; Peebles et al. 1989; Matarrese et al. 1997) is not treated here, apart from discussion of a possible high redshift, high initial bias in §5.3.

In interpreting the w estimate via integration of the relativistic version of Limber's equation, the size of galaxy dark matter haloes is explicitly considered. The effective three-dimensional separations studied here, i.e. the median separation of galaxy pairs which contribute to 50% of the projected correlation, is $r_{\rm eff}^{50\%}\approx 25{\rm h}^{-1}$ kpc$-250{\rm h}^{-1}$ kpc (Roukema & Valls-Gabaud 1997). Dark matter haloes must overlap at these length scales and it seems likely that some modification of the shape of the correlation function is necessary, since the dominant physics in coexistence of galaxy pairs becomes local rather than cosmological.

The simplest correction seems to be to introduce a smooth cutoff in ξ below a characteristic halo radius. This is the approach adopted here (§3.2.3).

The resulting estimates of w are presented in §4.1. In §4.2, these are interpreted in terms of the spatial correlation function with and without a correction for halo radii, for a range of simple power law hypotheses for correlation evolution with redshift, and for a realistic range in values for the cosmological curvature parameters, Ω_0 and λ_0.

Comparison with and implications from other estimates of ξ, in particular regarding the decreasing correlation period (DCP), are provided in §5, and §6 concludes.

The Hubble constant used here is $h \equiv H_0/$ 100km s^{-1} Mpc^{-1}. The spatial correlation function is presented in comoving coordinates. Galaxy halo sizes are discussed in proper units. The metric parameters Ω_0 and λ_0 are quoted when first used (Fig. 10).

2 OBSERVATIONAL DATA SET

The HDF is presented in detail by Williams et al. (1996). Selection of galaxies in the U-band (strictly speaking, in the F300W band) for the three Wide Field Camera (WFC) fields of the HDF is described in Mobasher & Mazzei (1998), and is estimated to be complete to $U < 27$ (U_{AB} magnitudes used here).

Photometric redshifts were calculated by Mobasher & Mazzei (1998) using template spectral energy distributions (SED's) derived from stellar evolutionary population synthesis models. These extend from the far-UV to 1mm, self-consistently include stellar emission, internal extinction and re-emission by dust, and include a range of metallicities. The synthetic SED's were constrained both by locally observed galaxies of different morphological types and by the HDF galaxies for which spectroscopic redshifts are available. The r.m.s. scatter between spectroscopic and photometric redshifts is estimated as 0.11.

It should be noted that due to the lack of strong breaks in the optical passbands, the uncertainties in photometric redshifts are generally greater within the $1.5 < z < 2.5$ interval than at lower and higher redshifts. This is not a problem for this analysis. Since only the projected correlation function is estimated, errors within the interval have no effect. Scattering in the redshifts at the low redshift end might have some effect, since although the numbers of galaxies are relatively lower, their autocorrelation is higher, than at high redshifts. Uncertainty at the high redshift end should be minimised by the U-band selection.

3 METHOD

3.1 Estimation of the Angular Correlation Function $w(\theta)$

3.1.1 Angular limits

Since variance on the scale of the sample can only be corrected by information external to the sample, the estimation of w at angles similar to the size of either a single WFC field or the combined field cannot statistically represent structure at that projected angular scale. The presentation of angular correlations up to 80″ (Villumsen et al. 1997) or 220″ (Connolly et al. 1998) can therefore be considered as providing investigations of individual examples of structure, which could be used to select samples of individual high redshift clustered structures (or voids).

Although that approach is not without interest, the goal here is for the study of the statistics of galaxy clustering, so

the upper limit in angles used for correlation estimates is $\approx 40''$, half the size of a single WFC field. Previous experience (Roukema & Peterson 1994) suggests that this is a conservative limit above which large scale variance should be excluded. For the I-band limited HDF sample of Villumsen et al. (1997), formal interpretation of the error bars of Villumsen et al.'s Fig. 1 shows that negative and positive offsets of $w(\theta_i)$ estimates at 25-80$''$ from the power law corrected fit are mostly more significant than positive offsets on small scales. An alternative fit of any reasonably smooth function through the points would not reduce what is most simply interpreted as large scale variance.

At small angular scales there is certainly no problem in confusion of faint sources for $\theta \gg 0.1''$; these are Hubble Space Telescope data. On the contrary, the limitation is physical. Colley et al. (1996, 1997) have pointed out a highly significant excess of object pairs separated by less than about $1''$ in the HDF. This corresponds to about $6h^{-1}$ kpc in separation perpendicular to the line-of-sight (to within a factor of two depending on the values of the metric parameters), in proper units. Roukema & Valls-Gabaud (1997) showed that if these objects were individual galaxies with a correlation similar to or higher than that of equation (1), but allowing for evolution and a wide range of acceptable parameters, then the measured strength of w would imply that their three-dimensional separations would typically be the same as the perpendicular separation, and a large majority of pair separations would be less than 15-30h^{-1} kpc (proper).

Colley et al. also point out that differential bolometric surface brightness dimming of $(1+z)^4$ for diffuse objects relative to $(1+z)^2$ for point sources implies that one should in fact *expect* high redshift optical imaging to split galaxies into clumps of objects such as H II regions.

While a component of the sub-arcsecond clustering detected by Colley et al. may well be real galaxy clustering [though highly biased as predicted by Ogawa, Roukema & Yamashita (1997), apparently detected by Steidel et al. (1998) and modelled by Bagla (1998)], the choice adopted here is to exclude this clustering. This is done (i) by setting a minimum angular separation of $2''$ down to which the correlation is estimated and (ii) considering objects separated by less than $0.5''$ as single objects. The second of these two limits has to be significantly smaller than the first in order to avoid introducing a bias.

In order to maximise signal to noise, large bins are adopted as in Roukema & Peterson (1994). The range 2-70$''$ is divided into six logarithmic bins, of which the first three are regrouped into a single bin in order to reduce the noise, and the largest angular bin is plotted but not used in for correlation estimates or integral constraint corrections. The range used for correlation estimates is therefore 2-39$''$.

3.1.2 Masking for Bright Sources

In any image of faint galaxies, even one such as the HDF which was designed to avoid containing any 'bright' galaxies (or stars), there are still some galaxies which are brighter than others. It is clear in the HDF (e.g. Fig. 8 of Williams et al. 1996) that there are some bright galaxies which occupy non-negligible fractions of the total solid angle. As is generally pointed out in angular correlation studies (e.g. Neuschaefer et al. 1991; Roukema & Peterson 1994), subtraction of the light from bright objects is imperfect, both due to the light profile only being a smooth approximation and due to the Poisson noise from the object adding to that of the sky. This implies that (a) background galaxies (or foreground dwarf galaxies) which ought to be detected after subtraction of the bright objects may be missed (due to being subtracted away) and (b) Poisson noise, real components of the bright object (e.g. a globular cluster or a knot of star formation if the bright object is a galaxy), cosmic rays or combinations of the three may be mistakenly detected as galaxies.

Estimating the angular correlation function depends critically on the selection criteria being constant across the whole field (or for the selection function to be known precisely enough to enable a weighting correction to be applied) and can be biased by either of these effects. Analyses of the HDF tend to be conservative in reducing the possibility of mistaking artifacts for galaxies, so the problem here is more likely to be (a) than (b).

In either case, the correction is to apply a 'mask' to regions around bright objects. In this study, use of the U-selected catalogue would be insufficient since the photometric redshift estimates require detection in all bands and so would be affected by bright objects in other bands. So, Williams et al.'s catalogue is used to mask out circular areas around all objects of limiting isophotal areas of greater than 10 sq.arcsec. These regions are excluded when distributing random points for use in equation (2).

3.1.3 Different Estimators for w

The estimation of the angular correlation function amplitude for small solid angle, faint surveys normally suffers from the problems of small numbers of galaxies, of a small signal-to-noise ratio and of correcting for variance in the number density of galaxies on the scale of the sample observed (also known as the integral constraint). In this sample, the numbers of galaxies are relatively small, compared to the numbers in typical magnitude/surface brightness limited ground-based surveys extending to faint magnitudes (e.g. Efstathiou et al. 1991; Neuschaefer et al. 1991; Pritchet & Infante 1992; Couch et al. 1993; Roukema & Peterson 1994; Infante & Pritchet 1995 and Brainerd et al. 1995).

However, the small angular size of the HDF implies that w can be estimated at angular separations of less than $10''$, where it is expected to give a stronger signal, so that the signal-to-noise ratio may be sufficiently high for a significant estimate.

The other problem is that of sample-scale variance which both (a) can introduce noise into the correlation estimate and (b) needs to corrected for in order to have a statistic which is significant in the limit of large angles.

(a) Provided that the amplitude of this variance is smaller than unity, the arguments of Hamilton (1993) on how the noise it introduces can be reduced to a quadratic term rather than a linear term become valid. Since the three WFC fields are best considered independently (the small increase in the number of pairs across the borders between does not seem to justify the possible systematic effects of that particular sub-sample of the total close pair distribution), a simple, order-of-magnitude estimate of the variance

is provided from comparison of galaxy numbers in the three fields.

Hamilton's equation (15), adapted for the angular correlation function, is then an estimator which minimises the noise contribution of this variance relative to other estimators such as that of Landy & Szalay (1993). Hamilton's estimator, expressed in conventional terms, is

$$w(\theta) = \frac{N_{gg} N_{rr}}{N_{gr}^2} - 1 \quad (2)$$

where N_{gg}, N_{rr} and N_{gr} are the numbers of galaxy-galaxy pairs, random point-random point pairs and galaxy-random point pairs respectively, separated in each case by an angle lying in the interval $[\theta, \theta + \Delta\theta]$. Landy & Szalay's estimator, in the same terminology, is

$$w(\theta) = \frac{N_{gg} - 2N_{gr} + N_{rr}}{N_{rr}} \quad (3)$$

The random points are points selected pseudo-randomly from a uniform distribution in a field of the same shape and size as that from which the galaxies are selected. This corrects for edge effects.

(b) Large-scale variance is not included in eq. (2). The common technique for re-introducing large-scale variance is to assume that w should be a power law of a given slope,

$$w(\theta) = A_w \theta^{1-\gamma} \quad (4)$$

where A_w is a free parameter and γ is that of eq. (1). The uncorrected estimates $\{1 + w(\theta_i)\}$ have a constant term added (or are multiplied by a constant factor) such that a power law of slope $1 - \gamma$ is obtained.

This assumption is that adopted by nearly all authors of faint galaxy angular correlation function analyses who do not have large enough fields to avoid having to make this integral constraint correction. Villumsen et al. (1997) and Connolly et al. (1998) adopt this technique, and assume $\gamma = 1.8$.

Some authors only make the assumption that w is a power law, and try to estimate both the amplitude and slope of the power law by χ^2 minimisation (e.g. Neuschaefer et al. 1991).

This assumption is obviously sensitive to any minor changes in the slope or the shape of the correlation function over this limited angular range. As reviewed by Peacock (1997), it is likely that ξ is not perfectly fit by a single power law. Either a double power law or a fitting function such as that of Hamilton et al. (1991) are likely to be closer to the intrinsic shape of ξ. The effective slope over a small range in angle may be different enough from the assumed value of γ to add significant systematic error to the amplitude estimate.

Moreover, this corrected formula reintroduces linear error terms into the estimate. Effectively, the estimator becomes

$$w(\theta) = \frac{N_{gg} - 2N_{gr} + N_{rr}}{N_{rr}} + C \quad (5)$$

for some constant C.

Hamilton presents a version of this equation, [his eq. (24)], which optimally corrects for the large-scale variance:

$$w(\theta) = \frac{N_{gg} - 2\overline{n_{\rm est}} N_{gr} + \overline{n_{\rm est}}^2 N_{rr}}{\overline{n_{\rm est}}^2 N_{rr}} \quad (6)$$

where $\overline{n_{\rm est}}$ is the mean number density estimated by some means external to the sample, divided by the number density of the sample itself.

It is clear that varying the value of C in eq. (5) is not equivalent to varying $\overline{n_{\rm est}}$ in eq. (6). Finding a best fit for $w(\theta)$, subject to the constraint that it has a certain shape and slope, will not give the same results in the two equations.

In addition, Hamilton suggests using large scale variance estimated from very large scales such as the cosmic microwave background measurements by COBE as the external constraint. However, the extrapolation over time and space from COBE measurements to the present work would obviously require numerous assumptions.

Since in the present case the three WFC fields are analysed independently, a simple way of estimating the $\overline{n_{\rm est}}$ in the present case is to use the mean density of the three fields as the value of $\overline{n_{\rm est}}$ to use in evaluating eq. (6) for any single field. This should correct for variance on a scale considerably larger than that of interest.

As is seen below, this results in a mean correlation function which is positive and consistent with a power law, *and additionally avoids having to assume that it should be a power law in order to make the correction.*

In principle, there should still be a bias from variance on yet larger scales, but without large-scale galaxy surveys at $z \sim 2$ there is no obvious way to make this correction directly from observational data, apart from adopting the conventional practice of assuming that $w(\theta)$ should be a power law of a given slope.

The uncertainty in the correlation estimates is itself estimated, for any angular bin, by the dispersion in the w estimates between the three WFC fields.

3.2 Relating ξ to w

3.2.1 Use of Redshifts in Limber's Equation

The angular correlation function (small angle approximation) is given by the the double integration of $\xi(r, z)$,

$$w(\theta, N_z) = \frac{\int dz\, N_z(z)^2 \int du\, \xi(r, z)}{\left[\int dz\, N_z(z)\right]^2} \quad (7)$$

where $z = (z_1 + z_2)/2$ and $u = z_1 - z_2$ parametrise the redshifts of two galaxies at redshifts z_1 and z_2, $r(z, u)$ is the spatial separation of the two galaxies, and $N_z(z) = {\rm d}N/{\rm d}z$ is the redshift distribution of the sample studied (Limber 1953; Phillips et al. 1978; Peebles 1980; Efstathiou et al. 1991).

In the present case, Connolly et al.'s (1998) method of modelling a redshift distribution by summing the individual photometric redshifts, represented as Gaussian distributions centred on the estimated values, where $\sigma_z = 0.11$, is adopted.

3.2.2 Low Redshift Contribution to Limber's Equation

However, as remarked upon by Roukema & Valls-Gabaud (1997), the physical scales of the function ξ which contribute to the angular signal need to be carefully considered.

In principle, the combination of very short length scales and very high correlations in the very low z component of the cone of observation can be a problem in the integration

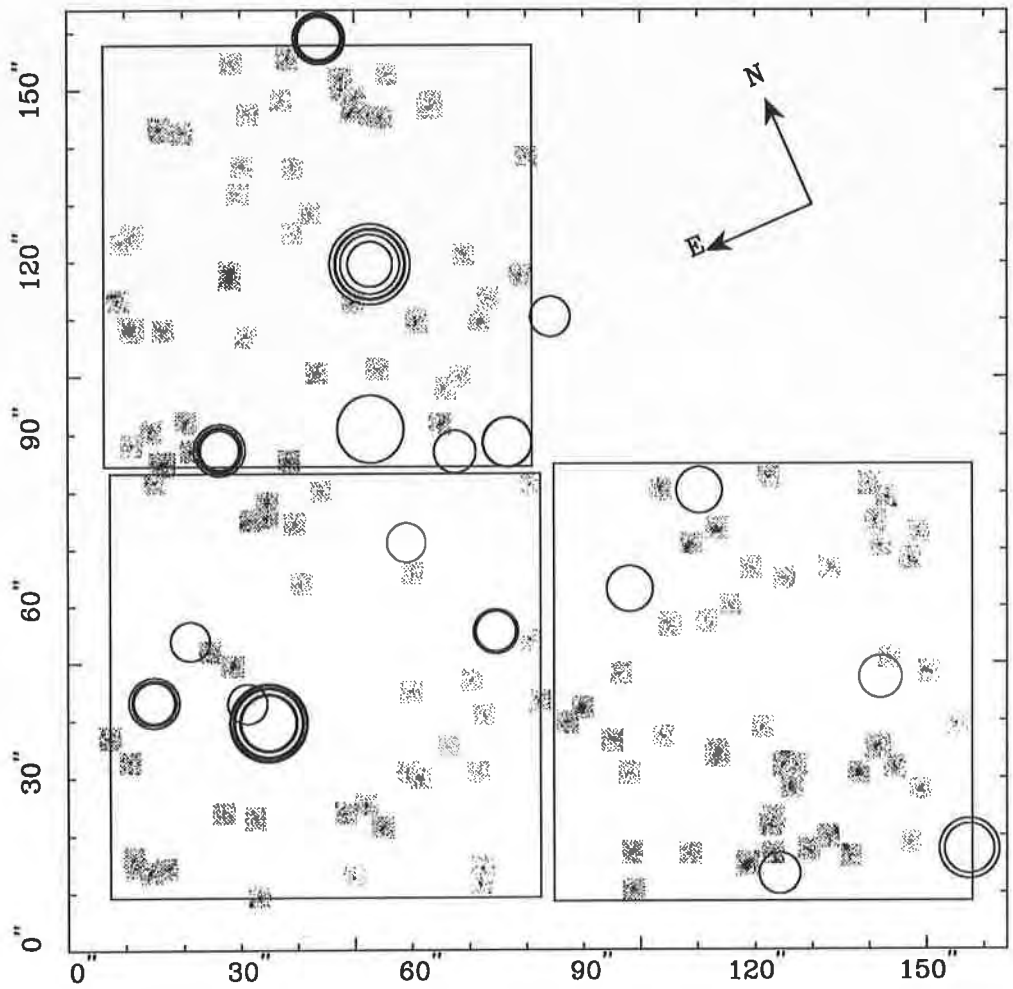

Figure 1. HDF U-selected $z \sim 2$ galaxies shown as $4'' \times 4''$ images extracted from the 1024 × 1024 pixel F300W mosaic of the HDF archive. The pixel scale is about 6.25 pix/$''$. North is to the upper left, east is to the lower left. Circles show areas excluded due to objects occupying large solid angles from which the $z \approx 2$ galaxies would not be selected in an unbiased way. Concentric circles indicate that Williams et al. (1996) chose various options for uniting bright 'split' galaxies; in such cases, the largest of the concentric circles is the effective exclusion zone here. The boundaries used by Mobasher & Mazzei (1998) are shown for the three WFC fields, labelled #2 (upper left), #3 (bottom left) and #4 (bottom right). One excluded area (circle) appears in the Planetary Camera field, which is not analysed.

of Limber's equation (whether analytical or numerical). This is because although the volume at low redshifts is small, the correlation modelled by a power law at small separations becomes extremely high*. The resulting contribution to w can be non-negligible (see Fig. 1, Roukema & Valls-Gabaud).

Although this could be considered to have some physical meaning, e.g. to represent the clustering of very faint ($U \lesssim 27$) dwarfs in the Local Group, the small angular size of the field ($\approx 4.5 \times 10^{-7}$ sr) implies that any celestial population of objects needs to have at least $\approx 2.8 \times 10^7$ objects over 4π sr in order to expect (in the mean) a single object in the HDF. So a few small dwarf spheroidals distributed on the scale of the local supercluster could possibly be present in the HDF, but the presence of a Local Group galaxy would only be due to a very rare event.

In the present case, the interest is in cosmological distances, so photometric redshift estimation excludes this very low redshift component — certainly in the calculation and most probably in the observational data.

* It was pointed out by Bruno Maillard (personal communication) that since the observer lives in a non-random point of space, i.e. in a group and local super-cluster, the correct modelling of the correlation should be even higher towards zero pair separations at near zero redshifts.

3.2.3 Galaxy Halo Sizes

Given the exclusion of low redshifts ($z \lesssim 1.5$), the minimum three-dimensional separation considered in the integral is not too different from the perpendicular separation at the median redshift of the redshift band $1.5 \lesssim z \lesssim 2.5$. The perpendicular separations over these redshifts are considerably

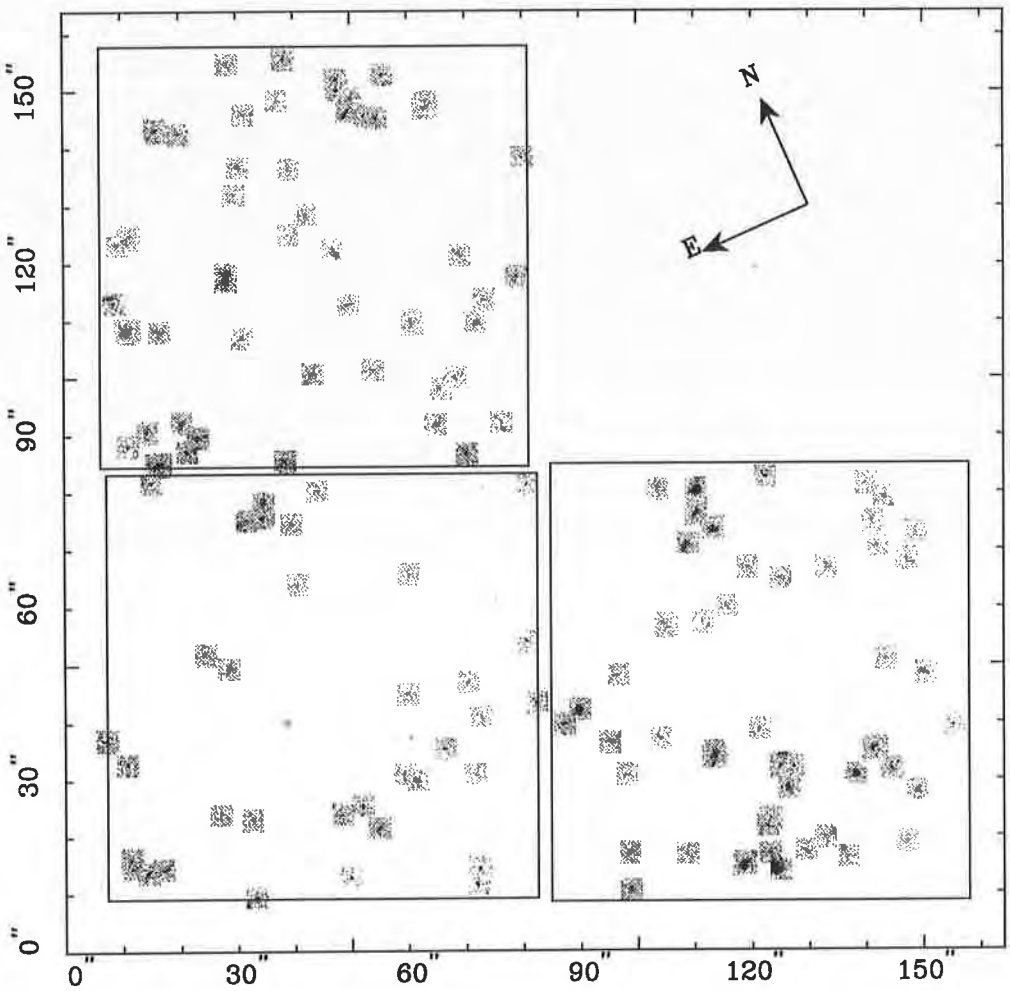

Figure 2. HDF U-selected $z \sim 2$ galaxies, as for Fig. 1 but without any masking of areas around large objects.

smaller than 100-200h^{-1} kpc, i.e. than likely present-day sizes of typical L^* galaxy haloes†.

Is it physically reasonable for galaxy pairs to exist as close to one another as 6h^{-1} kpc for long enough to have a chance of being observed in an HDF-like sample?

Hierarchical galaxy formation models would imply that galaxy haloes should be smaller at $z \sim 2$ than at the present. However, at typical redshifts of Lyman-α and metal line absorbers in front of quasars, the haloes of galaxies are estimated as having gaseous radii of around 50-200h^{-1} kpc (Bergeron & Boissé 1991; Bechtold et al. 1994; Lanzetta et al. 1995; Fang et al. 1996; Le Brun et al. 1996; Chen et al. 1998).

It is dynamically unlikely that the dark matter halo radii could be smaller than the gaseous radii, so the closest fit between theory and observation would be for dark matter halo radii to be about the same size as the gaseous radii.

It could be possible that the $z \sim 2$ galaxies in the HDF are mostly dwarfs (defined by mass), brightened by bursts of star formation, and that the types of galaxies corresponding to quasar absorbers are very rare in the HDF. In this case, galaxies could indeed coexist according to an extrapolation of ξ to small pair separations. Alternatively, since the half-light radii of HDF galaxies are small, it could be possible that the baryonic, stellar cores of haloes, i.e. galaxies, are tightly enough bound that they co-orbit in the haloes (i) without merging over a Hubble time and (ii) they do this is such a way that their pair separations remain statistically well modelled by ξ.

However, it seems reasonable that a fair fraction of the HDF galaxies, which are detected in spite of $(1+z)^4$ bolometric surface brightness dimming, have halo radii (gaseous and dark matter) in the 50-200h^{-1} kpc range.

Once gaseous haloes overlap, it is likely that in some fraction of cases (e.g. low relative velocities), these haloes will merge in much less than a Hubble time. Among the halo pairs that merge, some fraction of their baryonic, 'galaxy' cores will also merge rapidly. This removes pairs from the pair distribution. So, the pair probabilities, hence ξ, should be lower than that expected from the low r extrapolation of ξ from its cosmological context.

It is interesting to note the argument of Bartlett & Blanchard (1996) that dynamical estimates (from the cosmic virial 'theorem') are consistent with dark matter halo radii larger than conventionally assumed, i.e. bounded below

† The word 'haloes' is used here in the galaxy formation sense of dark matter haloes containing baryonic and/or nonbaryonic non-luminous matter.

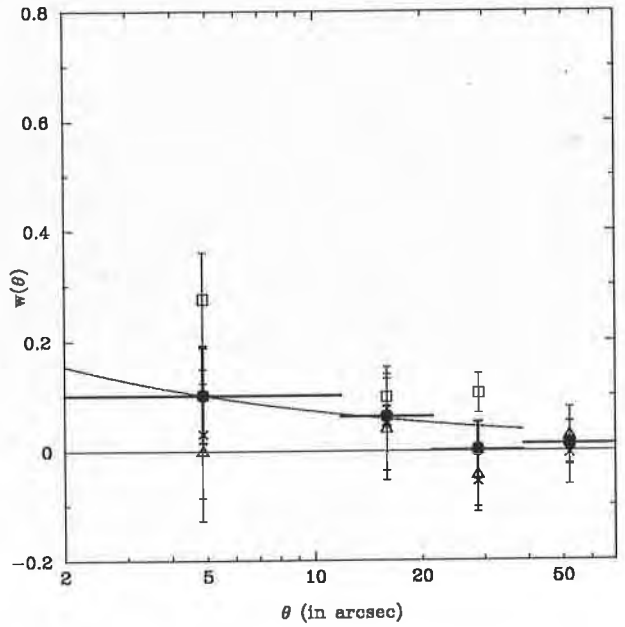

Figure 3. Angular correlation function w shown as a function of angle θ for the three WFC fields, shown as crosses (chip #2), squares (chip #3) and triangles (chip #4), using eq. (24) of Hamilton (1993) to estimate w, where $\overline{n_{\rm est}}$ is the mean number density of the fields (eq. 6 here) and where regions occupied by large objects are masked. Error bars on these points are Poissonian. The filled circles and their vertical error bars (in bold) show the mean values of w for the three chips considered as independent samples and the standard errors in the mean. Horizontal error bars show the bin sizes. A power law fit to the mean values is shown. See Table 1 for key numerical values in this and following figures.

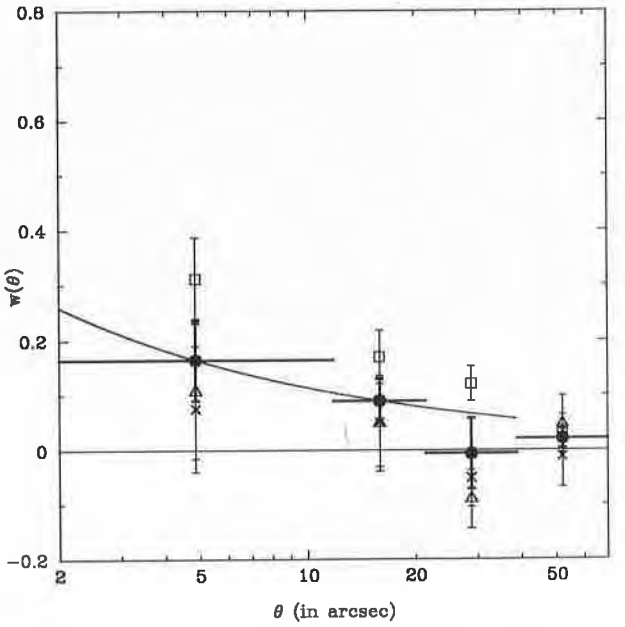

Figure 4. As for Fig. 3, but without any masking for regions around bright objects.

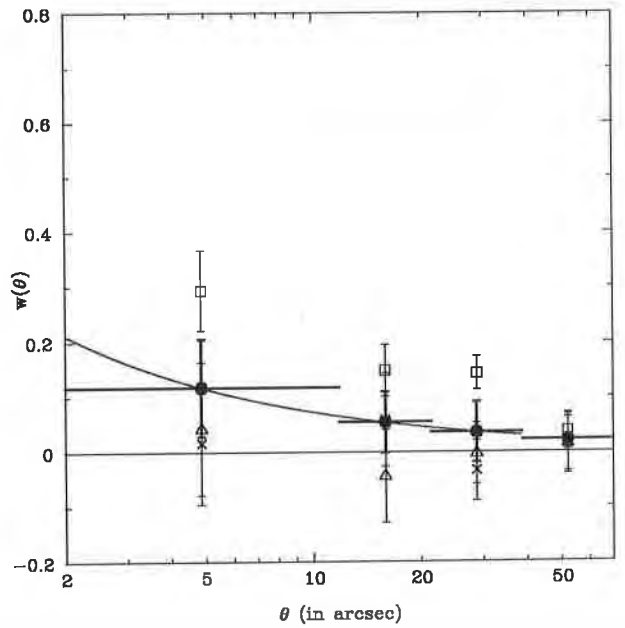

Figure 5. As for Fig. 3, but without any merging of close objects.

by $300h^{-1}$ kpc. However, there is no indication that matter extending out to these large radii would be baryonic, i.e. collisional, so rapid merging of pairs would be unlikely. In such a scenario, the expression 'halo radius' could be replaced by 'halo impact parameter leading to rapid merging'.

Many possible effects of pair exclusion are probably convolved, but the observational constraints are weak. So, the correction adopted here is simply to include a cut-off in ξ by a single parameter representing a 'typical halo radius', $r_{\rm halo}$. We consider how this affects the interpretation of the observed values of w. The cutoff is modelled smoothly as

$$\xi' \equiv \xi \times \begin{cases} 1, & r/(1+z) \geq r_{\rm halo} \\ \exp\left\{-\frac{[r_{\rm halo}-r/(1+z)]^2}{2\sigma^2}\right\}, & r/(1+z) < r_{\rm halo} \end{cases} \quad (8)$$

where $r_{\rm halo}$ is in *proper* units, $r/(1+z)$ is the proper separation corresponding to r in comoving units, and $\sigma = r_{\rm halo}/2$. This is a Gaussian cutoff, so that the probability of a pair of galaxies existing at $r/(1+z) = r_{\rm halo}/2$ is multiplied by $e^{-1/2} \approx 0.61$, and that of a pair at $r/(1+z) = r_{\rm halo}/10$ is multiplied by $e^{(-9/5)^2/2} \approx 0.20$.

4 RESULTS

Galaxies in Mobasher & Mazzei's (1998) HDF catalogue which have redshifts estimated as $1.5 \leq z \leq 2.5$ are shown in Fig. 1, for apparent magnitudes $23 \leq U_{\rm F300W} \leq 27$, over which the catalogue should be complete. Galaxies in areas biased by large objects are excluded. The galaxy positions are those of Mobasher & Mazzei, the galaxy images are from the the HDF archival F300W image and Williams et al.'s (1996) catalogue is used for the positions of large objects.

To be conservative, objects detected at less than

$$\theta_{\rm mask} \equiv 2\sqrt{A/\pi}, \quad (9)$$

from the centre of a large object, where $A = 10$ sq.arcsec is the solid angle within the isophotal limit of the large object, are excluded. Williams et al.'s catalogue includes several estimates of the isophotal areas for the brightest objects, depending on how many components of what seems to be a

Table 1. Estimates of amplitude and slope of $w(z \approx 2, 2'' < \theta < 40'')$ for different techniques. Columns show number of galaxies N_g; the assumption **A** for re-introducing large scale variance being either **A**= N, a constraint by $\overline{n_{\rm est}}$, or **A**= γ, a constraint by assumption of a power law of slope $1-\gamma$; the value of $1-\gamma$ assumed for parameters present in later columns; effective angle $\theta_{1-\gamma}$ (weakly dependent on assumed slope); $w(\theta \approx 5'')$ and its standard error in the mean $\sigma_{\overline{w}}$ estimated free from power law assumptions using eq. (24) of Hamilton (1993); an upper limit to $(1-\gamma)^+$ for a power law fit to the same derivation and its uncertainty; $w(\theta \approx 5'')$ and 1σ uncertainties based on the estimator of Landy & Szalay (1993); $w(\theta \approx 5'')$ and 1σ uncertainties based on eq. (15) of Hamilton (1993). The values of w are linear, not logarithmic. The first two lines are for masking of large objects, the second two without masking.

N_g				**A**	$(1-\gamma)$	$\theta_{1-\gamma}$	Hamilton (1993) eq. (24)				LS (1993)		Ham (1993) eq. (15)	
tot	#2	#3	#4				$w(\theta)$	$\sigma(\overline{w})$	$(1-\gamma)^+$	$\sigma[(1-\gamma)^+]$	$w(\theta)_{1-\gamma}$	$\sigma[w(\theta)_{1-\gamma}]$	$w(\theta)_{1-\gamma}$	$\sigma[w(\theta)_{1-\gamma}]$
Masking:														
142	55	35	52	N			0.10	0.09	−0.47	0.56				
142	55	35	52	γ	−0.7	5.5					0.20	0.11		
142	55	35	52	γ	−0.8	5.3	0.16	0.10	−0.96	0.27	0.19	0.10		
142	55	35	52	γ	−0.9	5.1					0.18	0.10		
Without masking:														
150	59	35	56	N			0.16	0.07	−0.51	0.44				
150	59	35	56	γ	−0.7	5.5					0.27	0.11		
150	59	35	56	γ	−0.8	5.3					0.26	0.10		
Without integral constraint correction ($C \equiv 0$):														
142	55	35	52	γ							0.09	0.08	0.12	0.11
Without merging of close objects:														
153	61	35	57	N			0.12	0.09	−0.66	0.55				
153	61	35	57	γ	−0.7	5.5					0.19	0.11		
153	61	35	57	γ	−0.8	5.3					0.18	0.10		

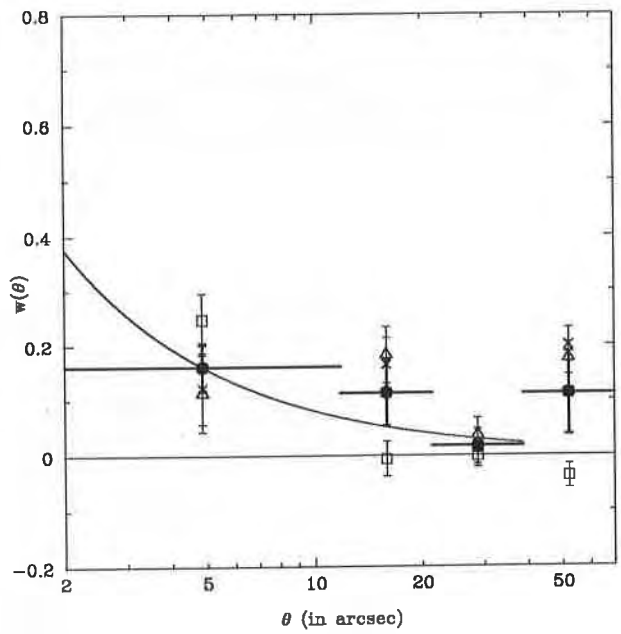

Figure 6. As for Fig. 3, but varying $\overline{n_{\rm est}}$ in order to best fit w to a power law with slope $1-\gamma = 0.8$. The slope of the curve shown is $1-\gamma = 0.85$.

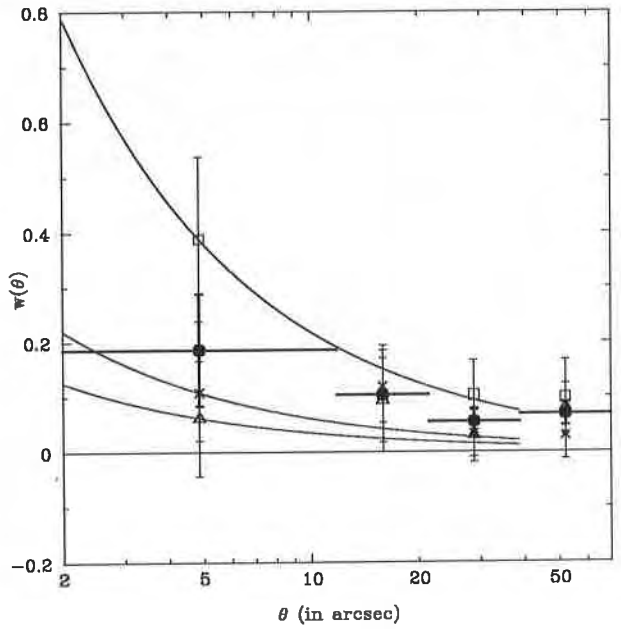

Figure 7. As for Fig. 3, except the calculation of w is based on Landy & Szalay's (1993) estimator plus an integral constraint additive correction (eq. 5) for individual fields such that the corrected correlations are power laws of slope $1-\gamma = -0.8$ (cf. Villumsen et al. 1997; Connolly et al. 1998). The power laws required for the corrections for the individual fields are shown. The mean values are calculated after the corrections.

single object are counted as a single one. This is seen as several concentric rings around a single bright object. The masked zone in such a case is defined by the largest ring.

Fig. 2 shows a similar image, but without any masked regions. It is clear by comparison of the two images that several of the 'voids' in this figure correspond to the larger of the masked regions in Fig. 1. This suggests that galaxies have been missed in these regions.

4.1 Estimates of w

Fig. 3 shows the angular correlation function estimated using eq. (6) for the selected galaxies shown in Fig. 1. Large-scale variance has been introduced via an estimate of $\overline{n_{\rm est}}$ 'external' to the sample, as recommended by Hamilton (1993), without making any assumption about the shape or

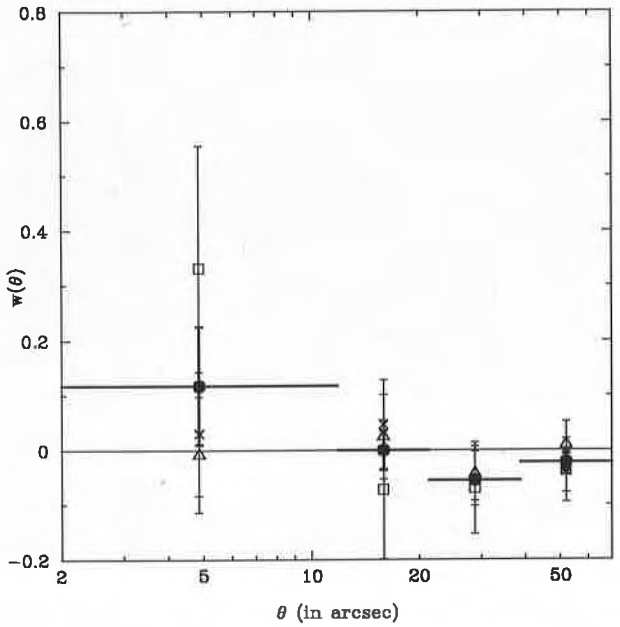

Figure 8. As for Fig. 3, but using eq. (15) of Hamilton (1993) [eq. (2) here].

slope of w This is done by considering the three WFC fields to be independent samples, and $\overline{n_{\rm est}}$ to be the global mean density for the three fields.

Strictly speaking, large scale variance at scales larger than the combined WFC fields would still be missing from our estimate of $\overline{n_{\rm est}}$. The standard deviation of the number of objects per WFC field is 10.8 (with masking and with merging of close objects), and the mean is 47.3, i.e. the standard error in the mean of the $\overline{n_{\rm est}}$ estimate is about 13%.

One way of potentially reintroducing the large scale variance is to follow the convention of fitting to a power law of a given shape and slope. This would only be correct if the true shape and slope are in fact those chosen. This is discussed further in §4.1.3.

The three fields, considered as independent samples, are averaged and the point in the lowest angular bin (at $\theta \approx 5''$) is considered to be the estimate of the amplitude of w. A fit to the three points in $2'' < \theta < 39''$ is considered as an upper limit to the slope $1 - \gamma$.

Table 1 lists numerical values for this estimate and for other estimates which take into account possible systematic errors and conventional estimators for w. The median angle in the $\theta \approx 5''$ bin is also listed. Since this depends on the slope $1 - \gamma$ and is only slightly higher than $5''$, the bin can be referred to as the '$5''$ bin' for brevity.

4.1.1 The Effect of Masking

Comparison of Fig. 3 and Fig. 4 shows that several 'voids' in the unmasked galaxy distribution shown in Fig. 2 correspond to masked areas shown in Fig. 1. This has a noticeable effect on w: the value increases by about 60% if the 'voids' are considered to be unbiased regions. The masked and unmasked values of $w(5'')$ are 0.10 ± 0.09 and 0.16 ± 0.07 respectively (Table 1).

Is the difference statistically significant? Suppose we consider the masked value, 0.10, to be the true value, the results of repeated experiments to be normally distributed about this with a standard deviation of 0.09, and the unmasked value, 0.16, to be a realisation of the same experiment. Then the null hypothesis that the unmasked value comes from the same experiment can only be rejected at a $P_{\rm Gauss}[(|w - 0.10|/0.09)\sigma < (0.06/0.09)\sigma] = 50\%$ confidence level. So it is not proven to high significance that objects have indeed been 'hidden' by the large objects.

The difference that does exist can be understood arithmetically as follows. An uncorrelated distribution punctuated by voids would become correlated; an already correlated distribution generally becomes more so. So, the effect is strongest for the two bins smaller than the typical 'void' size, as expected.

4.1.2 The Effect of Object Multiplicity

The effect of object splitting is small. Fig. 5 shows w estimated as in Fig. 3, but by considering objects separated by less than $0.5''$ as genuinely independent galaxies. If a single galaxy is seen as, say, multiple H II regions, which are wrongly assumed to be independent galaxies, than the correlation function would in effect be weighted more strongly by (a) galaxies close to these 'multiple galaxies' and (b) pairs of such 'multiple galaxies'.

Effect (a), on small scales, would be noticeable if the multiple galaxies are located in clustered regions, in which case they pair up with close galaxies. The multiplicity may be due to either the 'halo building blocks' or the 'H II region' interpretations.

If the multiplicity is due to the 'halo building blocks' model, then the 'multiple galaxies' would be in clustered regions, since there is no sharp cut in the hierarchy of clustering. In this case, effect (a) should be expected.

On the other hand, in the 'H II region' interpretation, due to $(1+z)^4$ bolometric surface brightness dimming, H II regions are favoured over disks relative to shot noise. In this case, there is no reason to expect these galaxies to be in clustered regions more often than 'non-multiple galaxies' are in clustered regions, apart from the extent to which star formation requires close galaxy-galaxy interactions and/or merging.

So the presence or absence of this effect would respectively favour the 'halo building block' or the 'H II region' interpretations of the sub-arcsecond pair excess noticed by Colley et al. (1996).

Effect (b) would be stronger as long as at least two 'multiple galaxies' are in the sample, since it would depend on the square of the r.m.s. multiplicity. If the multiple objects are relatively rare, the effect would occur at relatively large separations. The effect would be to increase the correlation at the separations of the multiple objects. If the multiple objects were common enough, then their contribution would reflect their intrinsic correlation as a population.

In this case, the multiple objects are rare: 6, 0 and 5 objects are doubly counted in the three fields respectively if objects separated by less than $0.5''$ are considered as independent real galaxies (see Table 1).

Hence, effect (b) is to be expected only at large scales and is separable from effect (a).

Between Figs 3 and 5, the effect is small in the $5''$ bin

and most obvious in the 21-39′ bin. This favours the 'H II' region interpretation, though not significantly.

4.1.3 Conventional Estimators

Villumsen et al. (1997) and Connolly et al. (1998) do not use an estimate of the mean density $\overline{n_{\rm est}}$ in order to include large-scale variance. They adopt the conventional technique of first estimating w with the mean density of the sample, then searching for an additive correction which best transforms the set of binned $\{w_i\}$ values close to a power law of slope $1-\gamma=-0.8$.

In the case of eq. (6), the only means of modifying this to fit a power law is to recalculate w for different values of $\overline{n_{\rm est}}$ until the closest resulting set $\{w_i\}$ to a power law of desired slope is obtained. The result obtained with the fixed 'external estimate' of $\overline{n_{\rm est}}$ gives a slightly shallower upper limit slope, $1-\gamma=-0.47\pm0.56$, than the conventional $1-\gamma=-0.8$. So, it could be expected that this more conventional constraint would give a slightly lower value for $w(5'')$, in order to increase the steepness of the slope.

However, this is not the case here; eq. (6) is not dependent on a simple additive parameter as is the case of eq. (5). Fig. 6 and the entry in Table 1 show that the closest slope to $1-\gamma=0.8$ attainable is $1-\gamma=-0.96$, and that $w(5'')$ increases from 0.10 to 0.16.

The formal significance of the difference obtained by using the power law constraint is (by coincidence) numerically the same as that if masking is omitted. That is, if the fixed constraint determines the true value of $w(5'')$, then the $1-\gamma=-0.8$ power law fit gives a value of $w(5'')$ rejected at only a $P_{\rm Gauss}[(|w-0.10|/0.09)\sigma<(0.06/0.09)\sigma]=50\%$ confidence level.

This is not equivalent to using eq. (5) with the same power law, as can be seen from the equations, from Fig. 7 and from Table 1. For the present data, eq. (5) overestimates w.

Again, consider 0.10 ± 0.09 to represent the true value and true error distribution, and consider the estimate from eq. (5) to be an unbiased realisation of this distribution. Then this null hypothesis is only rejected at a $P_{\rm Gauss}[(|w-0.10|/0.09)\sigma<(0.09/0.09)\sigma]=68\%$ confidence level.

However, as mentioned above, not all large scale variance is restored by using the mean of the three WFC fields to estimate $\overline{n_{\rm est}}$. So, an alternative is to consider the power law corrected estimate using eq. (6) to be the true estimate, restoring the large scale variance. In that case, the (power law corrected) estimate from eq. (5) considered as a realisation of the same experiment can be rejected only at a $P_{\rm Gauss}[(|w-0.16|/0.10)\sigma<(0.03/0.10)\sigma]=24\%$ confidence level.

This is not at all a significant difference, which is not surprising. The differences between the two formulae are in the linear error terms, so should be of the same order of magnitude as the uncertainties.

An advantage of eq. (5) is that for a typical data set, uncorrected correlations [$C=0$ in eq. (5)] are close to zero at large angles. This gives a good chance of being able to find a best fit power law as close as possible to the desired slope, since $C=0$ gives a very steep slope, $C\gg1$ gives a very shallow slope, and the effect should be smooth and continuous.

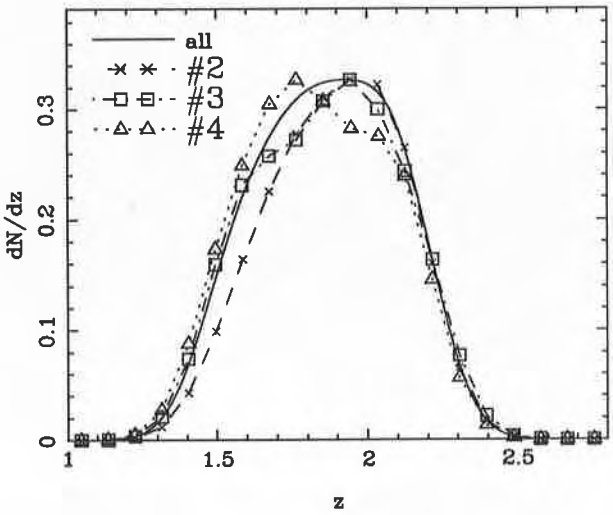

Figure 9. The photometric redshift distribution of the $1.5<z<2.5$ U-selected HDF galaxies for the individual WFC fields and in total (normalised).

This is equally a disadvantage, since the desired slope is attained even though the equivalent calculation, avoiding linear terms, using eq. (6), shows that this should not be the case, apart from consideration of the uncertainties. In other words, the desired slope is attained through inclusion of linear error terms, which is obviously less than optimal.

So that readers can compare with other works, the results of using eq. (5) for various assumed slopes and including the effects of not masking, of setting $C=0$ and of not merging close objects are also listed in Table 1.

For completeness, the application of Hamilton's eq. (15) [eq. (2) here], which avoids large scale variance altogether, is shown in Fig. 8. The missing variance is clear at the larger angles here.

4.2 Interpretations in Terms of ξ

4.2.1 Redshift Dependence

Although the purpose of this paper is less ambitious than the study of evolution of the correlation function, eq. (1), the redshift range under study is large enough that a simple power law model [in $(1+z)$] of spatial correlation evolution needs to be discussed. The following evolutionary version of eq. (1) is therefore adopted:

$$\xi(r)=(r_0/r)^{\gamma}(1+z)^{-(3+\epsilon-\gamma)} \qquad (10)$$

(Groth & Peebles 1977), with r and r_0 in comoving coordinates as before, and ϵ a factor representing evolution.

As argued by Peacock (1997), a double power law may provide a more observationally and theoretically justified fit, or as shown by Hamilton et al. (1991), a rational polynomial fitting function based on dark matter only N-body simulations can provide a theoretically justified model.

Given the uncertainties in the HDF data, it seems prudent to simply adopt the power law model. Moreover, since the clustering is at a strongly non-linear scale, it should be expected that it is stable in proper units, in which case eq. (10) with $\epsilon=0.0$ should be a fair approximation. This is

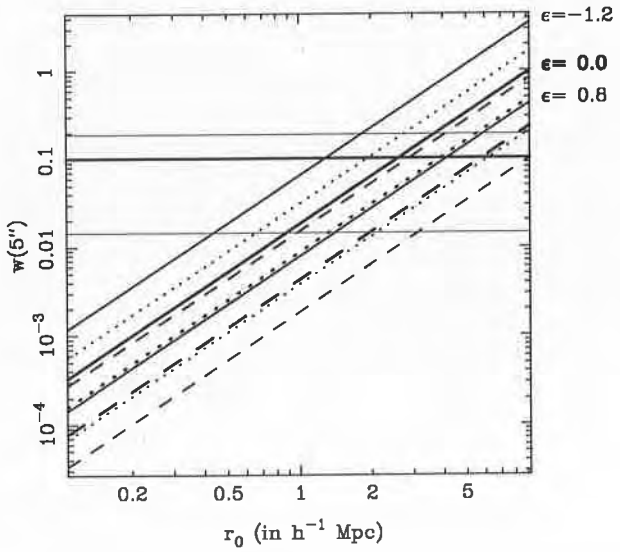

Figure 10. Angular correlation function amplitude $w(5'')$ calculated using eq. (7) and eq. (10) for a cutoff in the spatial correlation function ξ at pair separations $\lesssim r_0$ [eq. (10)], shown against r_0 in h^{-1} Mpc. The three sets of curves from top to bottom are for correlation evolution parameters $\epsilon = -1.2, 0.0$ and 0.8 respectively. Solid, dotted and dashed curves are for metric parameters $(\Omega_0 = 1, \lambda_0 = 0)$, $(\Omega_0 = 0{,}1, \lambda_0 = 0)$ and $(\Omega_0 = 0.1, \lambda_0 = 0.9)$ respectively. The photometric redshift distribution of the $1.5 < z < 2.5$ U-selected HDF galaxies (Fig. 9) is used in the integrals of eq. (7). The HDF estimate of $w(5'')$ obtained using eq. (24) of Hamilton (1993) (Fig. 3) is reproduced here by the horizontal lines, mean in bold, error bar as thin lines. $1 - \gamma = -0.8$ is adopted.

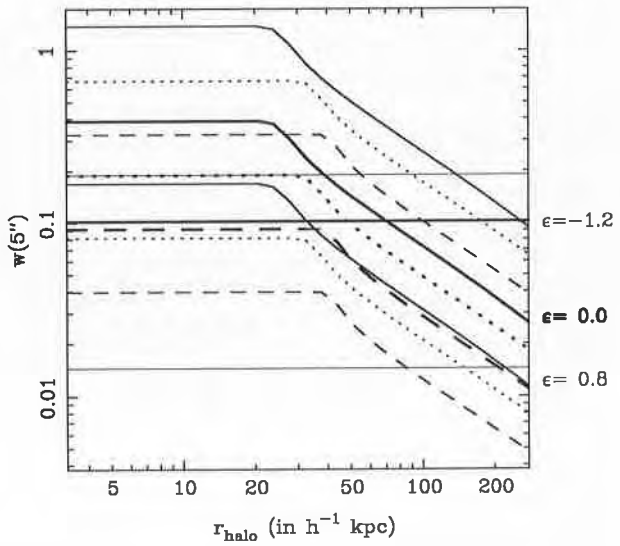

Figure 11. Angular correlation function amplitude $w(5'')$ calculated using eq. (7) and eq. (10) for a smooth cutoff in the spatial correlation function ξ at pair separations $\lesssim r_{\rm halo}$, in h^{-1} kpc, [eq. (8)] to take into account the non-zero size of dark matter halo radii. The present-day correlation length is fixed to $r_0 = 5.5h^{-1}$ Mpc. Other parameters and line styles are as for Fig. 10.

the possibility discussed primarily here, though other possibilities such as the inclusion of the effects of bias could, in principle, also be considered.

Other possibilities for correlation function evolution include $\epsilon = \gamma - 3$ (stable clustering in comoving coordinates), $\epsilon = 0.8$ (linear growth for $\Omega_0 = 1, \lambda_0 = 0$) and higher values for ϵ in the transition zone between linear and non-linear regimes.

The smoothed redshift distribution of Mobasher & Mazzei's catalogue is shown in Fig. 9. For the differences in the correlations between the three WFC fields to be attributed to redshift evolution, this would have to be in the sense of stronger correlations at higher redshifts (Ogawa et al. 1997). Noise within the error bars shown would be a more conservative interpretation.

4.2.2 Zero Redshift Correlation Lengths r_0

The correlations at redshift zero for proper length stable clustering (and for two other values of ϵ) are shown in Fig. 10 for $1 - \gamma = -0.8$. As is well known (Yoshii, Peterson & Takahara 1993), lower values of w are expected for low density and for low density Λ-dominated metrics than for an $\Omega_0 = 1, \lambda_0 = 0$ universe.

The $w(5'')$ estimate for this 'no-evolution' model is equivalent to $r_0 = 2.6^{+1.1}_{-1.7}h^{-1}$ Mpc $(\Omega_0 = 1, \lambda_0 = 0)$, $r_0 = 3.9^{+1.6}_{-2.6}h^{-1}$ Mpc $(\Omega_0 = 0.1, \lambda_0 = 0)$ or $r_0 = 5.8^{+2.4}_{-3.9}h^{-1}$ Mpc $(\Omega_0 = 0.1, \lambda_0 = 0.9)$.

The high density metric implies about 2σ inconsistency with low redshift estimates of $r_0 \sim 5.5h^{-1}$ Mpc (e.g. Davis & Peebles 1983; Loveday et al. 1992), but the low density metrics are clearly consistent with proper length stable clustering.

4.2.3 Halo Radius Cutoff

If the non-zero size of halo radii is taken into account, using eq. (8) and $r_0 = 5.5h^{-1}$ Mpc the measured value of $w(5'')$ implies halo characteristic radii which are very reasonable. This can be seen in Fig. 11

For clustering stable in proper units and this fixed value of r_0, halo radii are $r_{\rm halo} = 70^{+420}_{-30}h^{-1}$ kpc $(\Omega_0 = 1, \lambda_0 = 0)$, $r_{\rm halo} < 350h^{-1}$ kpc (1σ upper limit; $\Omega_0 = 0.1, \lambda_0 = 0$) and $r_{\rm halo} < 210h^{-1}$ kpc (1σ upper limit; $\Omega_0 = 0.1, \lambda_0 = 0.9$). Because no pairs of galaxies can be seen at less than the separation perpendicular to the line of sight, $r_{\rm halo}$ has no effect below a certain value, so for low density metrics only upper bounds are found.

These numbers are totally consistent with estimates from quasar absorption systems, if these are samples of a similar population of objects, of which some fraction merge quickly once the gaseous haloes overlap.

If the $w(5'')$ value estimated from the HDF had been much lower, say, a factor of ten lower, then the halo radii would have been considerably higher. By extrapolation, they would have been $r_{\rm halo} = 680^{+3700}_{-310}h^{-1}$ kpc, $r_{\rm halo} = 500^{+3160}_{-240}h^{-1}$ kpc and $r_{\rm halo} = 300^{+2010}_{-140}h^{-1}$ kpc respectively for the three metrics, suggesting larger galaxy exclusion radii than the estimated sizes of the absorption systems.

4.2.4 Angular Dependence of $w(\theta)$

The angular dependence of w might be thought to have a low θ cutoff in the presence of a non-zero value of $r_{\rm halo}$.

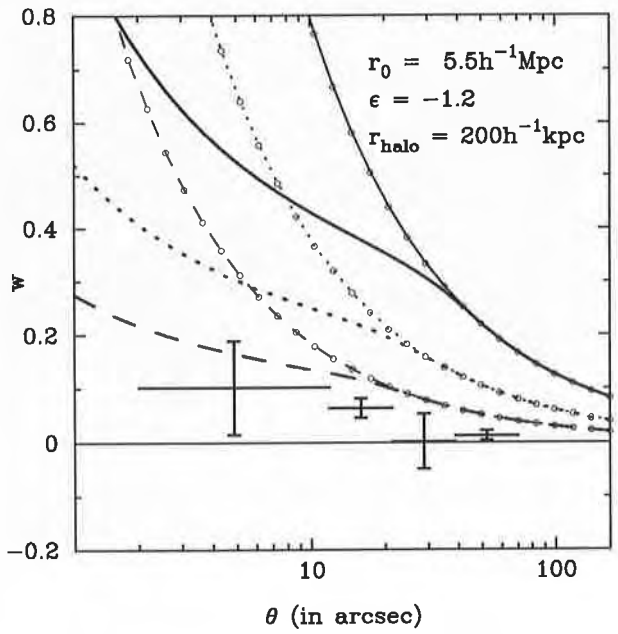

Figure 12. Angular correlation functions with and without a halo cutoff of $r_{\rm halo} = 100{\rm h}^{-1}$ kpc, for clustering stable in proper units. Different line styles are for different metric parameters as in Fig. 11. Thick lines are calculated with the halo cutoff, thin lines without. The circles are simply $1-\gamma$ power laws extrapolated from the right-hand side of the plot. Our HDF estimates obtained using eq. (6) are also shown.

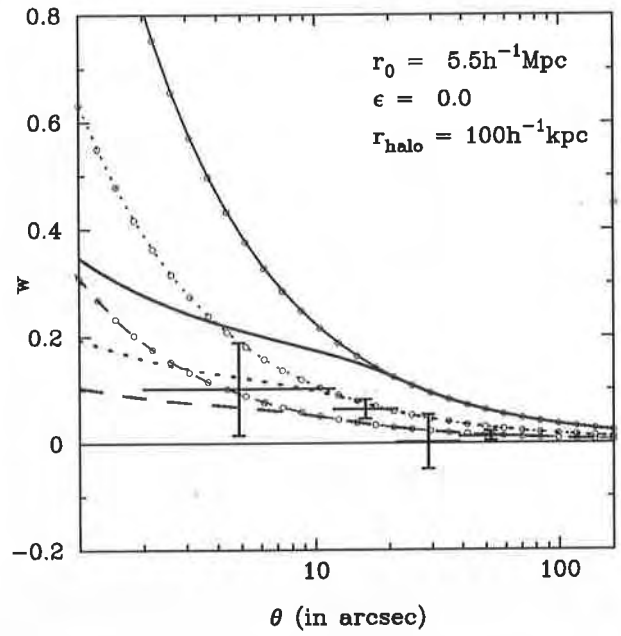

Figure 13. As for Fig. 12, but for clustering stable in comoving coordinates ($\epsilon = \gamma - 3$) and for $r_{\rm halo} = 200{\rm h}^{-1}$ kpc.

Fig. 12 shows that this is not the case. A simple round number of $r_{\rm halo} = 100{\rm h}^{-1}$ kpc was chosen for illustration, for the three choices of metric and no clustering evolution in proper units. This cutoff clearly has an effect. However, because w is a projection of ξ, pairs of galaxies separated by $r/(1+z) > r_{\rm halo}$ and whose separation vectors are oriented towards the line-of-sight are seen with perpendicular separations less than $r_{\rm halo}$, so there is still a strong signal.

This figure also shows that the high density metric model provides a less good fit than expected solely from considering $w(5'')$ as an amplitude estimate. An $r_{\rm halo} = 100{\rm h}^{-1}$ kpc halo size brings it into nearly 1σ consistency with the $w(5'')$ estimate, but it is inconsistent with the 12-21″ bin.

Of the three metrics used for the figure, the low density metrics provide the best fits. Since perpendicular distances for a given redshift and angle are smaller for these metrics than for a high density one, the effect of $r_{\rm halo}$ becomes negligible.

Alternative ways to best fit all points would be to increase ϵ to a value higher than that for stable clustering in proper units, i.e. $\epsilon > 0$ (e.g. Efstathiou et al. 1991; Brainerd et al. 1995), or to consider a bias factor (e.g. Ostriker 1993).

However, the uncertainties shown in the amplitudes of $w(\theta)$ in the figure are only statistical uncertainties. The differences in Figs 3-8 suggest that systematic uncertainties in the second and third bins could be too large for detailed comparison of different metrics or models of bias.

How strong could the effect of $r_{\rm halo}$ could be? For stronger evolution with redshift than $\epsilon = 0$, the expected values of w would be lower than in Fig. 12, so non-zero $r_{\rm halo}$ would either have a statistically insignificant effect or would imply lower values than observed.

A lower limit to evolution is that of clustering which is constant in comoving coordinates. Fig. 13 shows this case, for a round value of $r_{\rm halo} = 200{\rm h}^{-1}$ kpc. This is sufficient to bring a high density metric model to within $\sim 3\sigma$ of the $w(5'')$ value, but it remains highly inconsistent with w at all larger angles. The Λ-dominated metric model is brought within the 1σ limit of the $w(5'')$ value, but still remains inconsistent at about 2σ with the 12-21″ bin.

5 DISCUSSION

How do these results compare with the other HDF analyses?

5.1 Comparison with Villumsen et al. (1997)

Table 1 of Villumsen et al. (1997) shows that their estimate of w which could be most closely compared to the present one would be for their $R < 29$ magnitude limited sample, which is modelled to have a median redshift of $z_{\rm med} \approx 1.9$, similar to that of our U-band plus photometric redshift selected sample. Since the redshift distribution of Villumsen et al.'s sample is much wider, a lower amplitude should be expected.

Their amplitude is equivalent to $w(5.3'') = 0.017 \pm 0.009$ (using the effective angle over our '5″ bin' for $1-\gamma = 0.8$). Because of the way that angular diameter changes with redshift, the three-dimensional separations probed by Villumsen et al.'s sample should not be very different from that of our sample. So, these separations should be mostly in the strongly non-linear regime, where no evolution in proper units is expected ($\epsilon = 0$).

Therefore, most of the difference in amplitude should come from the effect of the superimposition of many 'independent' slices, each intrinsically auto-correlated ($\xi_{ii} = \xi$)

but having zero correlation with other slices ($\xi_{ij} = 0$). An order of magnitude estimate of this effect would be to take the half-maximum points of the redshift distribution in Fig. 9 as the limits of dN/dz used here, i.e. $1.6 \lesssim z \lesssim 2.2$, to take $z_{\rm med}/2$ and $3z_{\rm med}/2$ as the limits of Villumsen et al.'s distribution for $R < 29$, and count the number of 'slices' of our sample that would fit in theirs (using comoving distance coordinates). The number of our 'slices' which would fit in theirs are $N = 3.4$-3.2 (depending on the metric parameters in the order listed above). Their correlation amplitude can then be summed over pairs of slices ij as

$$\sim \frac{N\xi_{ii}+N(N-1)\xi_{ij}}{N^2\xi_{ii}} = \frac{N\xi_{ii}}{N^2\xi_{ii}} = \frac{1}{N} \qquad (11)$$

times our value, i.e. around 1/3.3 times ours.

In fact, their w value is about 1/7 of ours, so would be equivalent to roughly half of ours if restricted to a single 'slice'. For $\gamma = 1.8$, this would imply that their inferred value of r_0 (for a given set of metric parameters and no proper coordinate evolution) would be $\approx 2^{-1.8} \approx 0.3$ times our value. For $\Omega_0 = 1, \lambda_0 = 0$, our estimate of $r_0 = 2.6^{+1.1}_{-1.7}{\rm h}^{-1}$ Mpc would become $r_0 = 0.75^{+0.3}_{-0.5}{\rm h}^{-1}$ Mpc.

Villumsen et al.'s Fig. 3 (left panel) suggests that their modelling via Limber's equation would imply about $r_0 \sim 1.8 \pm 0.5{\rm h}^{-1}$ Mpc for $\Omega_0 = 1, \lambda_0, \epsilon = 0$, so this rough estimate from eq. (11) underestimates the integrated value by less than half an order of magnitude.

The ratio between Villumsen et al.'s r_0 value and ours is about a factor of 0.7. Although this disagreement is only significant at $\sim 1\sigma$, and the two data sets are selected quite differently, both data sets do consist of HDF galaxies, so it is worth commenting on possibilities for a systematic rather than random error.

Villumsen et al. have 1559 galaxies; we have 142. Villumsen et al. clearly have an advantage in numbers which should reduce Poisson error.

They also have the property of selecting galaxies in rest-frame wavelengths much closer to those of major low redshift galaxy surveys than of our U-selected sample. This would be an advantage if $z \sim 2$ galaxies were statistically similar to low redshift galaxies, but less so if a large proportion of $z \sim 2$ galaxies are either starbursting galaxies or ellipticals with UV upturns.

Villumsen et al. also have the disadvantage of combining galaxies of widely differing redshifts, which should increase noise, and of not knowing the precise shape of the redshift distribution. This could very easily provide a systematic error of a factor of 0.7 in r_0, e.g. see Fig. 2 [panel (a)] and Fig. 3 of Roukema & Valls-Gabaud (1997).

Other possible systematic uncertainties are the inclusion of linear uncertainty terms and the correction for regions obscured by large objects. Villumsen et al. used eq. (5) rather than eq. (6) and adopted the power law of slope $1 - \gamma = 0.8$ constraint. They did not refer to masking for bright objects.

5.2 Comparison with 'Low' Redshift Samples

Connolly et al.'s (1998) w estimates are based on photometric redshifts of 926 $U_{\rm F814W} < 27$ galaxies in the HDF and $0.4 < z < 1.6$. For $\epsilon = 0$, over the range $0.2 < \Omega_0 < 1, \lambda_0 \equiv 0$, the authors infer $r_0 \approx 2.8 \pm 0.3$ [1σ error, from their Fig. 3(a)].

This is close to our best estimate for $\Omega_0 = 1, \lambda_0 = 0$, but lower by 0.4σ than our result for $\Omega_0 = 0.1, \lambda_0 = 0$ (§4.2.2, using our uncertainty). So even without knowing what value of Ω_0 corresponds to their best estimate for r_0, their result is consistent with ours. The caveats regarding the use of eq. (5) and not correcting for regions biased by large objects also apply here.

Other correlation function estimates based on either spectroscopic or photometric redshifts include those of Le Fèvre et al. (1996) (spectroscopic, $z_{\rm med}$= 0.53) and Giavalisco et al. (1998) (spectroscopic, $z_{\rm med}$= 3.0) and Miralles et al. (1998) (photometric, $z_{\rm med}$= 3.7).

The first two of these estimates are for fields of angles about a factor of ten larger than that of an WFC field, so cover the transition scale between the quasi-linear and non-linear regimes of galaxy clustering and may not express clustering fixed in proper units. Nevertheless, we discuss these briefly.

Le Fèvre et al.'s $z_{\rm med}$= 0.53 result for the present-day value of r_0 and $\epsilon = 0$ (§4.1-1. of Le Fèvre et al. 1996) is $r_0 = 3.0 \pm 0.2{\rm h}^{-1}$ Mpc ($\Omega_0 = 1, \lambda_0 = 0$) or $r_0 = 3.9 \pm 0.2{\rm h}^{-1}$ Mpc ($\Omega_0 = 0.2, \lambda_0 = 0$). This is consistent with our result. However, this is likely to be a coincidence. The effect of a non-zero size of $r_{\rm halo}$ which can decrease the inferred r_0 on the HDF scale studied by Villumsen et al., Connolly et al. and ourselves, is replaced in the case of Le Fèvre et al., by clustering growth stronger than $\epsilon = 0$ which decreases the values of r_0 at low redshifts (cf. §5.3).

It should be kept in mind that the galaxies in our sample (Mobasher & Mazzei 1998) are selected at rest wavelengths of around 1000Å, so comparison with correlation functions estimated for low redshift galaxies is difficult. Mobasher & Mazzei find that the galaxies in the sample are mostly ellipticals and starburst galaxies.

At low redshifts, the former have slightly higher correlations than the general galaxy population.

If the latter are a random selection of young disk galaxies which have just collapsed and started a rapid burst of star formation, then the corresponding correlation implied from low redshifts should be slightly lower than that of the total population. On the other hand, if only those young disk galaxies which happen to be close to one another have star bursts in order to be selected among our HDF 'UV drop-in' sample, then the correlation could well be higher.

Modelling the combination of the two populations would also require knowledge of the cross-correlation between them.

So, the overall population mix observed at $z \sim 2$ is likely to represent a complex mix of the populations at low redshifts. The different effects might cancel each other out, or cause a significant systematic effect.

5.3 The Decreasing Correlation Period

Giavalisco et al.'s result at $z_{\rm med}$= 3.0 for Lyman break galaxies (LBG's) is for a large value of r_0. Expressed as values for clustering fixed in proper units [i.e. multiplying by $(1+z_{\rm med})^{[0-(\gamma-3)]/\gamma}$] this is $r_0 = 5.3^{+1.0}_{-1.3}{\rm h}^{-1}$ Mpc ($\Omega_0 = 1, \lambda_0 = 0$) or $r_0 = 8.4^{+1.8}_{-1.5}{\rm h}^{-1}$ Mpc ($\Omega_0 = 0.2, \lambda_0 = 0$). This is about 2σ larger than our estimate.

As these authors discuss, this seems to be a detection of the decreasing correlation period (DCP; Roukema 1993; Brainerd & Villumsen 1994; Ogawa et al. 1997; Bagla 1998; Steidel et al. 1998; Moscardini et al. 1998; Coles et al. 1998). The DCP is the period of large galaxy formation when the transition from linear perturbations to non-linear collapsed haloes may have caused a high bias factor in the initial correlation function of these haloes, which later disappeared as perturbations in underdense regions also collapsed.

Since most of the signal in w of Giavalisco et al. is for $\theta > 20''$, this is corresponds mostly to larger length scales than our measurements. Their point which appears to be for a 0-20″ bin (Fig. 2 their paper) is lower than their power law fit, so they may not have a detection of the DCP at this scale.

Nevertheless, the DCP is clearly absent at the small scales measured in this paper from the HDF. Following Ogawa et al. (1997), a simple power law extension of eq. (10) is

$$\xi(r,z) = \begin{cases} \left[\frac{(1+z)}{(1+z_t)}\right]^{\nu} \xi(r,z_t), & z > z_t \\ (r_0/r)^{\gamma}(1+z)^{-(3+\epsilon-\gamma)}, & z_t \geq z > 0 \end{cases} \quad (12)$$

where correlation evolution and parameters for low redshift are as for eq. (10), but a transition redshift z_t and DCP slope ν parametrise the evolution during the DCP.

If the present study does not miss the DCP due to the smallness of the length scale studied, then our result combined with that of Giavalisco et al. would imply that z_t lies somewhere in the range $2 < z_t < 3$.

This would imply that the transition from the stage of the first collapse of large haloes in high density regions to the stage when most haloes of the same mass scale have collapsed finishes just before the time of major star formation (cf. Madau et al. 1996). Corrections to Madau et al.'s plot for dust (e.g. Mobasher & Mazzei 1998; Hughes et al. 1998) would imply an earlier and less sharply peaked maximum in the volume-averaged star formation history, so the overlap between the two epochs would seem to be even stronger. That is, the major star formation period would start just when most haloes of large mass have collapsed.

Finally, we consider the analysis of Miralles et al. (1998) for HDF galaxies at $z_{\rm med}$= 3.73. The measured correlation function for these galaxies is less easy to interpret than that of the present paper. The most significant correlation is in the bin centred at $\theta \approx 30''$. This could either be (a) a clustered region occurring by chance at this particular redshift, or (b) a detection of the DCP to a slightly higher redshift than that of Giavalisco et al.. Expressed for an $\Omega = 1, \lambda = 0$ universe and $\epsilon = 0$, the correlation length is $r_0 = 7.1 \pm 1.5 {\rm h}^{-1}$ Mpc (Miralles et al. 1998).

That is, the amplitude is higher than that of Giavalisco et al. (1998), expressed in terms of the same parameters. Since it is at a higher redshift this is just what would be expected from the DCP.

If we take the two estimates together as estimates of the initially highly biased correlation above that expected for clustering fixed in proper coordinates, adopt 1σ uncertainties of $\delta(z_{\rm med}) = 0.1$ for the two data sets, and use $1-\gamma = -0.8$, then the value of ν in eq. (12) is $\nu = 2.1 \pm 3.6$. Moreover, if we consider our result and that of Connolly et al. (1998) to be the 'stable' non-linear correlation length achieved at the end of the DCP, $r_0 \sim 2.6 \pm 1.4$, then the transition redshift marking the end of the DCP is $z_t = 1.7 \pm 0.9$.

This is clearly consistent (within the error bars) with the lack of detection of the DCP in the present work. That is, the extrapolation of a simple power law evolution through the estimates of Miralles et al. (1998) and of Giavalisco et al. (1998) implies that the DCP finishes just slightly below $z = 2$, i.e. has mostly disappeared by the epoch of our estimate.

In addition, these values happen to lie well within the constraints derived from diverse N-body models (§3, §6, Ogawa et al. 1997).

However, since the Giavalisco et al. result is for larger scales, it would be more consistent to compare the two at scales for which stable clustering in proper units may not be valid, in which case the analysis would be a lot less trivial than the simple estimate made here.

5.4 Halo Radii

Our value of $r_0 = 2.6^{+1.1}_{-1.7} {\rm h}^{-1}$ Mpc is lower than typical low redshift values of $r_0 \sim 5 {\rm h}^{-1}$ Mpc. As shown in §4.2.3 and §4.2.4, for $r_0 = 5.5 {\rm h}^{-1}$ Mpc and $\epsilon = 0$, the correction for halo pair exclusion implies very reasonable values of $r_{\rm halo}$ to match the measured value of $w(5'')$.

Matching the 12-21″ bin in addition (if ignoring systematic uncertainties), would require a low density metric, a higher value of ϵ or a moderate anti-bias, in which case the correction for non-zero 'halo radii' is likely to be considerably smaller for the present data set.

Could the effect of $r_{\rm halo}$ be detected in other data sets ? Both Fig. 5 of Miralles et al. (1998) and Fig. 3 of Postman et al. (1998) show decreases in slope below around 30″ and 60″ respectively, which are qualitatively similar to those in Fig. 12 and Fig. 13.

In Fig. 12, the effect of $r_{\rm halo} = 100 {\rm h}^{-1}$ kpc could be expected to occur below angles corresponding to perpendicular (proper) distances of $100 {\rm h}^{-1}$ kpc, i.e. 14-24″ for the three sets of metric parameters. It is clear that the effect, integrated precisely via Limber's equation, occurs just slightly below these angles.

In that case we can estimate the values of $r_{\rm halo}$ below which values of w falling below a projected $1 - \gamma = -0.8$ power law could be explainable simply by our halo cutoff formula. The angles in Fig. 5 of Miralles et al. (1998) and Fig. 3 of Postman et al. (1998) at which these falloffs occur (in the latter just the two fainter slices are considered) would imply values of $r_{\rm halo}$ just slightly larger than 100-$210 {\rm h}^{-1}$ kpc and 250-$360 {\rm h}^{-1}$ kpc respectively.

The former is reasonable. The latter is rather large, and for 'halo exclusion' to apply, would require an explanation of why galaxies rarely occur close to each other (relative to the expectation from a power law ξ) at $z \sim 0.8$, but are able to occur this closely for long enough periods at lower redshifts, such that the effect disappears in Postman et al.'s analyses for brighter magnitudes.

Low redshift estimates of ξ at short separations would be good for comparison, but few exist. Davis & Peebles (1983) analysis is consistent with eq. (1) on scales $10 {\rm h}^{-1}$ kpc $\lesssim r \lesssim 10 {\rm h}^{-1}$ Mpc, but the correlations are quite noisy at the small scales of interest. A more recent estimate is that of Tucker et al. (1997), who finds a similar result down to about $20 {\rm h}^{-1}$ kpc, but for the redshift-space corre-

lation function rather than the 'real' (i.e. spatial) correlation function, so this also is not easy to interpret.

6 CONCLUSIONS

We have estimated the amplitude of the angular two-point galaxy auto-correlation function $w(\theta)$ for galaxies at $z \sim 2$ from a a $U < 27$ complete sub-sample of the HDF, and find a result compatible, though slightly higher, than that of Villumsen et al. (1997), although the two samples have similar estimated median redshifts. The use of photometric redshifts, the avoidance of linear error terms in the estimator used for calculating the correlation function and the masking of regions biased by large objects favour our result as the more accurate of the two estimates; but the smallness of the numbers of galaxies in our sample favours that of Villumsen et al. as the more precise.

The consistency between the two samples suggests that the high star formation rate and domination by starburst galaxies and ellipticals in our U-band selected sample compensates for any effects due to the difference in rest-frame wave-bands between our sample and other samples. Since U-band selection also has the advantage of a good high redshift cut-off and helps to estimate photometric redshifts, this seems a useful strategy to complement selection in other wavebands. The technique could be referred to as the 'UV drop-in' technique (cf. Steidel et al. 1996).

(i) Use of eq. (6), i.e. eq. (24) of Hamilton (1993), is illustrated in observational data, possibly for the first time. It is shown how this compares to the use of eq. (5). Both equations are similar to that of Landy & Szalay 1993, but eq. (6) corrects for uncertainty in the mean number density, $\overline{n_{\rm est}}$, without re-introducing linear error terms.

The estimate using eq. (6) requires an external estimate of $\overline{n_{\rm est}}$, which we estimate from the mean of the three WFC fields, considering the individual fields as independent experiments (but with identical selection criteria). This gives $w(\theta \approx 5'') = 0.10 \pm 0.09$. Alternatively, adoption of the conventional constraint that w should be a power law of a given slope, for $1-\gamma = -0.8$, increases this by 60%, but the desired slope cannot be exactly obtained. Given the former estimate and its uncertainty, the possibility that the latter is identical to the former is only rejected at a 50% confidence level. Since the variance is related to the uncertainty, it is unsurprising that the difference is not formally of high significance.

Eq. (5), which requires an assumption about the shape and slope of w, and which is normally sure of obtaining this slope, implies values about twice as high as these, depending on what value of $1-\gamma$ is assumed. This can be rejected at the 68% confidence level given a true value and error distribution as estimated using eq. (6) and $\overline{n_{\rm est}}$ from the mean of the three fields. However, relative to the estimate from constraining eq. (6) to a power-law of the same slope, this is only rejected at the 24% confidence level. Again, the differences are related to the uncertainty terms, so are of a similar order of magnitude.

(ii) Biases introduced in faint galaxy selection by large objects, in this case by what appears to be the 'hiding' of galaxies by Poisson noise, creating 'voids', increases the estimate cited by 60% if it is not corrected. The null hypothesis of not masking introducing no change is rejected only at the 50% confidence level.

The difference in estimates of w with and without merging together of objects closer to one another than $0.5''$ is negligible at $5''$, though is noticeable at larger angles. This favours (marginally) the 'H II region' interpretation of sub-arcsecond HDF galaxy pairing relative to the 'building blocks' interpretation (see Colley et al. 1996, 1997).

(iii) The scales effectively studied here are in the range $\approx 25{\rm h}^{-1}$ kpc$-250{\rm h}^{-1}$ kpc, so overlapping of gaseous and/or dark matter haloes should exclude some fraction of galaxy pairs. A simple formalism for correcting ξ by a smooth (Gaussian) cutoff [eq. (8)] is presented. For clustering stable in proper units [$\epsilon = 0$ in eq. (10)] in an $\Omega = 1, \lambda = 0$ universe, our $w(5'')$ estimate (a) implies a present-day correlation length of $r_0 \sim 2.6^{+1.1}_{-1.7}{\rm h}^{-1}$ Mpc if halo sizes are ignored, but (b) for a present-day correlation length of $r_0 = 5.5{\rm h}^{-1}$ Mpc implies that a typical halo radius is $r_{\rm halo} = 70^{+420}_{-30}{\rm h}^{-1}$ kpc.

This value of $r_{\rm halo}$ is comfortably close to what could be expected, although this correction was not devised to fit the present data. It was pointed out by Roukema & Valls-Gabaud (1997) as simply being a correction likely to be needed just because halo and galaxy sizes are nonzero.

However, comparison of $w(\theta)$ as integrated using Limber's equation with that estimated for the $z \sim 2$ galaxies shows that this correction is insufficient to bring an $\Omega = 1, \lambda = 0$ universe into agreement with the data for clustering stable in proper units. Indeed, the second bin has a more significant estimate of w than the first, if only statistical uncertainties are considered: $w(\approx 16'') = 0.063 \pm 0.018$. However, comparison of Figs 3-8 shows that systematic uncertainties are probably a few times larger than the statistical uncertainties for this (and larger) bins.

In the case of a cosmological constant dominated universe ($\Omega_0 = 0.1, \lambda_0 = 0.9$), $r_{\rm halo}$ has little effect, and as is already well known for previous estimates of w (e.g. Yoshii et al. 1993), a good fit over all angles results for low density metrics and $\epsilon = 0$, with or without a cosmological constant to flatten the metric. Higher values of ϵ or anti-bias should have similar effects. However, the systematic uncertainties in the larger angular bins imply that a detailed fit across all angles may not be justified.

It should also be noted that the lack of an internal correction for sample variance is a common feature of all the HDF angular correlation function estimates, because of the HDF's small size. This introduces uncertainty in all of these estimates. For the lowest redshift samples, a power law constraint based on large solid angle, faint apparent magnitude/surface brightness limited samples could provide an observationally justified way to reduce this error. For the objects at successively higher redshifts, surveys using UV drop-in and UV drop-out techniques over large solid angles could provide observational estimates of the large scale variance.

(iv) The results of Giavalisco et al. (1998) and Miralles et al. (1998) can be expressed, for an $\Omega = 1, \lambda = 0$ universe and $\epsilon = 0$, as zero-redshift correlation lengths of $r_0 = 5.3^{+1.0}_{-1.3}{\rm h}^{-1}$ Mpc and $r_0 = 7.1 \pm 1.5{\rm h}^{-1}$ Mpc respectively. These are both strongly suggestive of a decreasing correlation period (DCP; Roukema 1993; Brainerd & Villumsen 1994; Ogawa et al. 1997; Bagla 1998; Steidel et al. 1998; Moscardini et al. 1998; Coles et al. 1998), during which

the first haloes to collapse do so in high density regions, so are highly biased relative to the underlying density perturbations. The period terminates when most haloes of the same mass scale, in both high and low density regions, have collapsed, so that the correlation function behaves 'normally', i.e. at small scales is stable in proper coordinates.

The decreasing correlation period (DCP) of a high initial bias in the spatial correlation function is not detected in our data, so would have to terminate in the range $2 \lesssim z_t \lesssim 3$.

A simple fit to the two values just cited for Giavalisco et al. and Miralles et al. would imply values of $z_t = 1.7 \pm 0.9$ and $\nu = 2.1 \pm 3.6$ in Ogawa et al.'s extension of the standard power law fit [eq. (12)]. That is, values of ξ at redshifts greater than $z_t = 1.7 \pm 0.9$ would be $[(1+z)/(1+z_t)]^{2.1 \pm 3.6}$ times their values at z_t, for a fixed value of r in comoving units.

These values are consistent with those estimated from N-body simulations (Ogawa et al. 1997) and with our lack of detection of the DCP.

However, since the three studies are optimised to different scales, and since Miralles et al.'s result might be that of an individual structure which is not statistically representative, this parametrisation of the DCP should be taken with caution.

ACKNOWLEDGEMENTS

This research has been supported by the Polish Council for Scientific Research Grant KBN 2 P03D 008 13 and has benefited from the Programme jumelage 16 astronomie France/Pologne (CNRS/PAN) of the Ministère de la recherche et de la technologie (France). Use has been made of the HDF archive of the Space Telescope Science Institute at *http://www.stsci.edu/ftp/science/hdf/archive/v2.html* and of the resources of the Centre de données astronomiques de Strasbourg (CDS).

References

Bagla J. S., 1998, MNRAS, 299, 417 (astro-ph/9711081)
Bartlett J. G., Blanchard, A., 1996, A&A, 307, 1
Bechtold J., Crotts A. P. S., Duncan R. C., Fang Y.-H., 1994, ApJ, 437, 83L
Bergeron J., Boissé P., 1991, A&A, 243, 344
Brainerd T. G., Smail I., Mould J., 1995, MNRAS, 275, 781
Brainerd T. G., Villumsen J. V., 1994, ApJ, 431, 477
Chen H.-W., Lanzetta K. M., Webb J. K., Barcons X., 1998, ApJ, 498, 77
Cole S., Ellis R., Broadhurst T., Colless M., 1994, MNRAS, 267, 541
Coles P., Lucchin F., Matarrese S., Moscardini L., 1998, MNRAS, 300, 183
Colley W. N., Rhoads J. E., Ostriker J. P., Spergel D. N., 1996, ApJ, 473, L63 (astro-ph/9603020)
Colley W. N., Gnedin O. Y., Ostriker J. P., Rhoads J. E., 1997, ApJ, 488, 579
Connolly A. J., Szalay A. S., Brunner R. J., 1998, ApJ, 499, L125
Couch W. J., Jurcevic J. S., Boyle B. J., 1993, MNRAS, 260, 241
Davis M., Peebles P. J. E., 1983, ApJ, 267, 465
Efstathiou G., Bernstein G., Katz N., Tyson J. A., Guhathakurta P., 1991, ApJ, 380, L47
Fang Y.-H., Duncan R. C., Crotts A. P. S., Bechtold J., 1996, ApJ, 462, 77
Giavalisco M., Steidel C. C., Adelberger K. L., Dickinson M. E., Pettini M., Kellogg M., 1998, ApJ, 503, 543
Groth E. J., Peebles P. J. E., 1977, ApJ, 217, 385
Hamilton A. J. S., 1993, ApJ, 417, 19
Hamilton A. J. S., Matthews A., Kumar P., Lu E., 1993, ApJ, 374, L1
Hughes D., et al., 1998, Nature, 394, 241 (astro-ph/9806297)
Infante L., Pritchet C. J., 1995, ApJ, 439, 565
Le Fèvre O., Hudon D., Lilly S. J., Crampton D., Hammer F., Tresse L., , 1996, ApJ, 461, 534 (CFRS-VIII)
Landy S. D., Szalay A. S., 1993, ApJ, 412, 64
Lanzetta K. M., Bowen D. B., Tytler D., Webb J. K., 1995, ApJ, 442, 538
Le Brun V., Bergeron J., Boissé P., 1996, A&A, 306, 691
Limber D. N., 1953, ApJ, 117, 134
Loveday J., Maddox S. J., Efstathiou G., Peterson B. A., 1995, ApJ, 442, 457
Madau P., Ferguson H. C., Dickinson M. E., Giavalisco M., Steidel C. C., Fruchter A., 1996, MNRAS, 283, 1388
Matarrese S., Coles P., Lucchin F., Moscardini L., 1997, MNRAS, 286, 115
Miralles J. M., Pelló R., Roukema B. F., 1999, astro-ph/9801062
Mobasher B., Mazzei P., 1998, ApJ, (submitted),
Moscardini L., Coles P., Lucchin F., Matarrese S., 1998, MNRAS, 299, 95
Neuschaefer L. W., Windhorst R. A., Dressler A., 1991, ApJ, 382, 32
Ogawa T., Roukema B. F., Yamashita K., 1997, ApJ, 484, 53
Ostriker J. P., 1993, AnnRevA&A, 31, 689
Peacock J. A., 1997, MNRAS, 284, 885
Peebles P. J. E., 1980, The Large-Scale Structure of the Universe (Princeton N. J., U.S.A.: Princeton University Press)
Peebles P. J. E., Daly R. A., Juszkiewicz, 1989, ApJ, 347, 563
Phillips S., Fong. R., Ellis R. S., Fall S. M., MacGillivray H. T., 1978, MNRAS, 182, 673
Postman M., Lauer T. R., Szapudi I., Oegerle W., 1998, astro-ph/9804141
Pritchet C. J., Infante L., 1992, ApJ, 399, L35
Roukema B. F., 1993, Ph.D. thesis, Aust.Nat.Univ.
Roukema B. F., Peterson B. A., 1994, A&A, 285, 361
Roukema B. F., Valls-Gabaud D., 1997, ApJ, 488, 524
Steidel C. C., Giavalisco M., Pettini M., Dickinson M. E., Adelberger K. L., 1996, ApJ, 462, L17
Steidel C. C., Adelberger K. L., Dickinson M. E., Giavalisco M., Pettini M., Kellogg M., 1998, ApJ, 492, 428
Tucker D. L., et al., 1997, MNRAS, 285, L5
Villumsen J. V., Freudling W., da Costa L. N., 1997, ApJ, 481, 578
Warren S. J., Iovino A., Hewett P. C., Shaver P. A., 1993, Observational Cosmology, (San Francisco, U.S.A.: Astr.

Soc. Pac.), p. 163.
Williams R. E., et al., 1996, AJ, 112, 1335
Yoshii Y., Peterson B. A., Takahara F., 1993, ApJ, 414, 431